Processing and Application of Ceramics 11 [4] (2017) 329–336
https://doi.org/10.2298/PAC1704329K

Mechanical properties of hot-pressed SiC-TiC composites

Kamil Kornaus*, Grzegorz Grabowski, Marian Rączka, Dariusz Zientara, Agnieszka Gubernat

AGH University of Science and Technology, Department of Ceramics and Refractories, Faculty of Materials Science and Ceramics, al. Mickiewicza 30, 30-059 Cracow, Poland

Received 3 March 2017; Received in revised form 5 September 2017; Received in revised form 21 November 2017; Accepted 11 December 2017

Abstract

SiC-TiC composites, with 0, 5, 10 and 20 vol.% of TiC, were sintered by the hot-pressing technique at temperature of 2000 °C under argon atmosphere. SiC sintering process was activated by liquid phase created by the reaction between Al_2O_3 and Y_2O_3, in which it is possible to dissolve passivating oxide layers (SiO_2 and TiO_2) and partially SiC and TiC carbides. Microstructure observation and density measurements confirmed that the composites were dense with uniformly distributed components. Differences in thermal expansion coefficients between SiC and TiC led to complex stress state occurrence. These stresses combined with the liquid-derived separate phase between grains boundaries increased fracture toughness of the composites, which ranged from 5.8 to 6.3 MPa·m$^{0.5}$. Opposite to the bending strength, fracture toughness increased with the TiC volume fraction. By means of simulation of residual thermal stresses in the composites, it was found that with the increasing volume fraction of TiC, tensile stress in TiC grains is reduced simultaneously with strong rise of compressive stresses in the matrix.

Keywords: *SiC-TiC composites, thermal stresses, mechanical properties, hot pressing, fracture toughness*

I. Introduction

Silicon carbide is characterized by interesting thermomechanical properties. It has very high hardness (~20 GPa), high wear resistance, high thermal conductivity coefficient and high oxidation resistance, but low fracture toughness. Moreover, it retains its hardness and bending strength at temperatures exceeding 1500 °C. Most valuable properties of silicon carbide arise from covalent bonds dominating in this material. On the other hand, dominating covalent bonds contribute to low self-diffusion coefficients, and by itself, lead to poor sinterability of SiC [1,2]. In addition, the attempts to obtain dense SiC polycrystals from fine powders by sintering supported by uniaxially and isostatically applied pressure were unsuccessful. It is well known [2–11] that use of sintering activators is essential for obtaining dense SiC materials, in both single phase polycrystals and SiC based composites.

There is a large group of composites with the SiC matrix and a second phase inclusions which do not impair properties such as hardness or thermal conduction and increase bending strength and fracture toughness [12–15]. SiC-TiC composites belong to this group and effective sintering activators of the SiC matrix are oxide additives such as a mixture of alumina (Al_2O_3) and yttrium oxide (Y_2O_3) in 3 : 2 mass ratio [3–8,11]. Usually, it is introduced into the SiC powder in the amount of 10–20 wt.% [11]. The Al_2O_3 to Y_2O_3 oxide mass ratio of 3 : 2 corresponds to the lowest melting eutectic (1760–1810 °C) in the Al_2O_3-Y_2O_3 system. The produced composites were characterized by only slight increase in fracture toughness (K_{Ic} = 4–5 MPa·m$^{0.5}$) as compared to the single-phase ceramics of SiC or TiC. Significant increase in fracture toughness was observed after prolonged annealing of composites at temperatures between 1900 and 2000 °C, which led to abnormal grain growth of SiC. The K_{Ic} coefficient of composites increased to almost 7 MPa·m$^{0.5}$ [16–18]. Improved fracture toughness is associated with the decrease of bending strength. The bending strength significantly depends on the annealing time. It decreased from 700 to 200 MPa after 12 h annealing of the sample containing 30 wt.% SiC - 70 wt.% TiC, while fracture tough-

* Corresponding author: tel: +48 513 442 371,
fax: +48 12 633 46 30, e-mail: *kornaus@agh.edu.pl*

Table 1. Characteristics of SiC and TiC powders

Property	SiC	TiC
content of C [%]	28.50–29.50	avg. 19.26
content of O [%]	max. 2.5	0.6
metallic impurities (Al, Ca, Fe) [%]	<0.10	<0.20
specific surface area [m^2/g]	23–25	-
average particle size [μm]	0.80	1.26

Table 2. Characteristics of SiC and TiC powders

Composite	Apparent density [g/cm^3]	Phase composition [wt.%]
SiC-0TiC	3.21 ± 0.01	91.8% SiC; 8.2% residual phases
SiC-5TiC	3.30 ± 0.02	84.2% SiC; 4.5% TiC; 11% residual phases
SiC-10TiC	3.39 ± 0.08	81.7% SiC; 12.9% TiC; 6.5% residual phases
SiC-20TiC	3.59 ± 0.05	70.2% SiC; 24.0% TiC; 5.8% residual phases

ness rose from 4.5 to 6.2 $MPa \cdot m^{0.5}$ [16]. Improvement of fracture toughness is correlated with the generation of the first type thermal stresses as well as the microstructure of composites. Intentionally initiated crack is bifurcated and deflected, moreover, crack bridging can be observed at elongated SiC grains. In turn, the higher amount of TiC the lower bending strength of composites is observed. This phenomenon results from the stronger thermal stresses which may lead to the creation of microcracks in the matrix, which are in turn responsible for decreasing bending strength. These stresses are stronger when matrix grains are larger, which explains significant decline of strength in composites after annealing [16–18].

Recently, attempts to produce SiC-TiC composites by SPS technique have been performed [19–21]. The application of the SPS technique avoids the use of SiC sintering activators and a significant reduction in the sintering temperature of 200–300 °C is noted. However, no significant improvement in the mechanical properties of composites was observed compared to the previously used sintering techniques. Interesting attempts to obtain SiC-TiC composites include pressureless sintering tests in which titanium carbide is formed *in situ* by carbothermal reduction of TiO_2 [22]. The relative density of such obtained composites is the highest, for low volume fraction of TiC, and reaches 94–98 TD%.

The paper presents investigations on mechanical properties and the simulation of residual thermal stresses in SiC-TiC composites, which were combined with qualitative and quantitative microstructure analysis. The composites were obtained by the hot-pressing technique. SiC sintering activators in the form of oxides were used. Based on these studies, an attempt was made to explain the effect of titanium carbide inclusions on the mechanical properties of composites, in particular on the fracture toughness.

II. Experimental procedure

The samples were prepared using sub-micrometric SiC (HC Starck UF 25) and TiC (ABCR GmbH & Co. KG AB122483) powders (Table 1). The oxide sintering activators in the form of Al_2O_3 (Timei TM-DAR, 99.9%) and Y_2O_3 (Boguchwała, 99.9%) were introduced in the 3 : 2 mass ratio, in amount of 10 wt.% in relation to SiC. The following four powder mixtures were prepared: SiC with 0, 5, 10 and 20 vol.% of TiC denoted as SiC-0TiC, SiC-5TiC, SiC-10TiC and SiC-20TiC, respectively. The mixtures were wet homogenized in an isopropyl alcohol for 12 h by means of the ball mill with the sintered SiC grinding media. Slurries were dried under the IR irradiation and then mixtures were granulated through perlon sieve. The samples were hot-pressed at 2000 °C/0.5 h, under 25 MPa pressure and argon flow.

Apparent density was measured by hydrostatic weighting method. Analyses of the sintered samples phase composition were performed by X-Ray diffraction technique (PANalytical Empyrean) and the obtained data were refined with the Rietveld method. In order to allow microstructure observation, metallographic sections were prepared (Struers Rotopol 25). Microstructures were observed using scanning electron microscope (Nova Nano SEM 200, FEI Company).

The hardness of the composites was measured by the Vickers method. In order to determine hardness of the composites, 10 indents under a load of 1 kg (9.81 N) were made. Single-edge-notched beam method was used to calculate fracture toughness (Zwick/Roell 2.5 kN). Bending strength was measured using three point bending test (Zwick/Roell 2.5 kN). The test specimens as well as bending strength and fracture toughness tests were performed in accordance with PN-EN ISO6872. In each case, measurements were performed on 6 samples.

III. Results and discussion

3.1. Phase composition and microstructure

The results of density and phase composition measurements of the composites are presented in Table 2. It can be seen that bulk density of the materials increases with TiC content. This phenomenon can be explained by an increase in the volume fraction of TiC, which has sig-

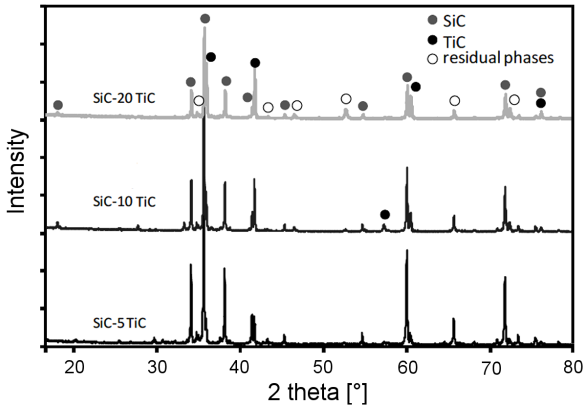

Figure 1. XRD analysis of SiC-TiC composites with 5, 10 and 20 vol.% TiC

nificantly higher density (4.92 g/cm^3) than the SiC matrix (3.21 g/cm^3). The XRD analysis of the composites confirmed the presence of two main phases, i.e. SiC and TiC, as well as phases produced by the reaction between the oxide activators (Fig. 1). Precise determination of the type and amount of phases resulting from the reaction between oxides or carbides and oxides is very difficult. On the basis of the most intense reflections, phases such as YAG (yttrium aluminum garnet) and YAM (yttrium aluminum monoclinic) are most probably present in the composites. However, the formation of aluminum or yttrium carbide and mixed carbides cannot be excluded. Due to the difficulty in accurately determining the type and number of residual phases it is also impossible to calculate the theoretical density and porosity of composites. However, it can be observed from the SEM

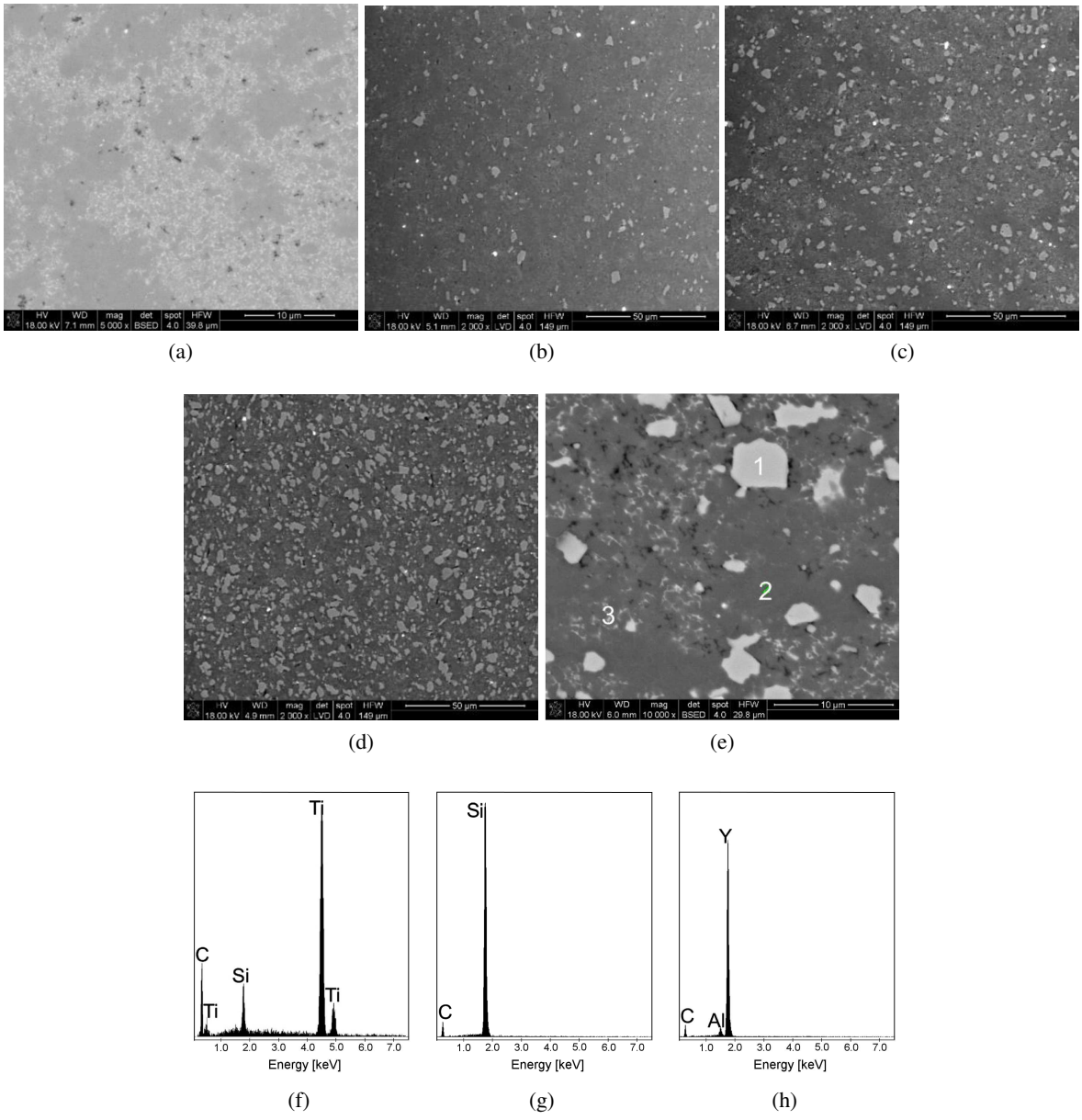

Figure 2. SEM micrographs of SiC-0TiC (a), SiC-5TiC (b), SiC-10TiC (c) and SiC-20TiC (d) composites and EDS point analysis of different sections of SiC-20TiC composite (e,f,g,h)

micrographs that the composites are dense (Fig. 2). Homogeneous distribution of TiC grains (light areas) in the SiC matrix (dark areas) was also noted (Fig. 2). Chemical analysis of composite micro-areas was performed by EDS analysis (Fig. 2f,g,h). Light phase network of residues of oxide activators can be observed between SiC grains, mainly at grain boundaries.

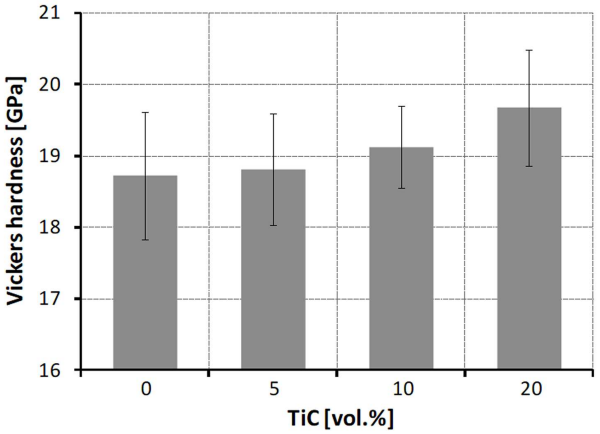

Figure 3. Vickers hardness of materials

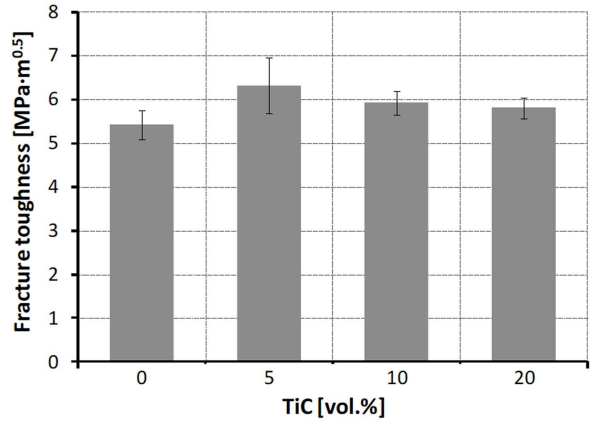

Figure 4. Fracture toughness of materials

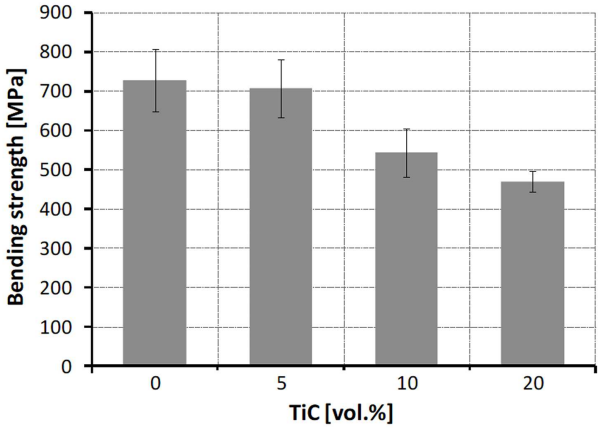

Figure 5. Bending strength of materials

3.2. Mechanical properties

The Vickers hardness of composites increased with TiC volume fraction (Fig. 3). This fact can be associated with the decreasing SiC volume fraction, thus, the volume fraction of oxide activators, whose residues and reaction products are visible in the microstructure. These phases have a significantly lower hardness (8–15 GPa) [23], as compared to both carbides, having similar hardness ~20 GPa [24,25].

Silicon carbide sintered with only oxide activators only exhibits the lowest fracture toughness, i.e. 5.3 MPa·m$^{0.5}$. For all composites, an increase in fracture toughness in comparison with the reference sample (SiC-0TiC) is observed (Fig. 4). The highest K_{Ic} of 6.3 MPa·m$^{0.5}$ has the composite with 5 vol.% TiC. The fracture toughness of the single-phase polycrystalline SiC, i.e. sintered with boron and carbon additives is 3.5–4.0 MPa·m$^{0.5}$ [1,24–26]. Similar or higher fracture toughness values of composites, up to 7.8 MPa·m$^{0.5}$, were obtained by prolonged annealing (2–12 h), under pressure, at high temperatures (1900–2000 °C), leading to strong unidirectional grains growth of SiC [15–17,27].

On the other hand, the bending strength declined from ~700 MPa for the silicon carbide without TiC additives and SiC-5TiC composite to ~450 MPa for the composite SiC-20TiC (Fig. 5).

The formation of residual thermal stresses, resulting from a large difference in thermal expansion coefficients between two carbides, are the possible cause of the fracture toughness increase and bending strength decrease. Verification of this hypothesis is explained later in section 3.3. Both carbides have isotropic thermal expansion coefficients α, which are $5.3 \cdot 10^{-6}$ and $7.4 \cdot 10^{-6}$ K^{-1} for SiC and TiC, respectively. Moreover, the residues of the oxide activators which occur at grain boundaries may reduce the strength of grain boundaries. The stresses as well as reduced strength of grain boundaries cause that emerging cracks extend between the grains, leading to their deflection and elongation (Fig. 6a,b). As expected, an effect of cracks bridging was observed (Fig. 6c,d) in the composites with 10 and 20 vol.% of TiC. All these phenomena have positive influence on the effective fracture energy improvement, thus, it increases the fracture toughness of composites.

3.3. Modelling

The finite element method (FEM) was used to calculate residual thermal stresses in the SiC-TiC composites. The geometric models were based on Representative Volume Element concept (RVE) [28,29]. It was assumed that the modelled area is a cube with dimensions of 10 × 10 × 10 μm, wherein the grains of inclusion are randomly distributed so as to obtain expected volume fraction (Table 3). Single grains, which filled RVE, had the shape of icosahedrons. Its size ranged from 0.1 to 2.0 μm. The position and orientation of the inclusions were random, and the grains could interpenetrate each

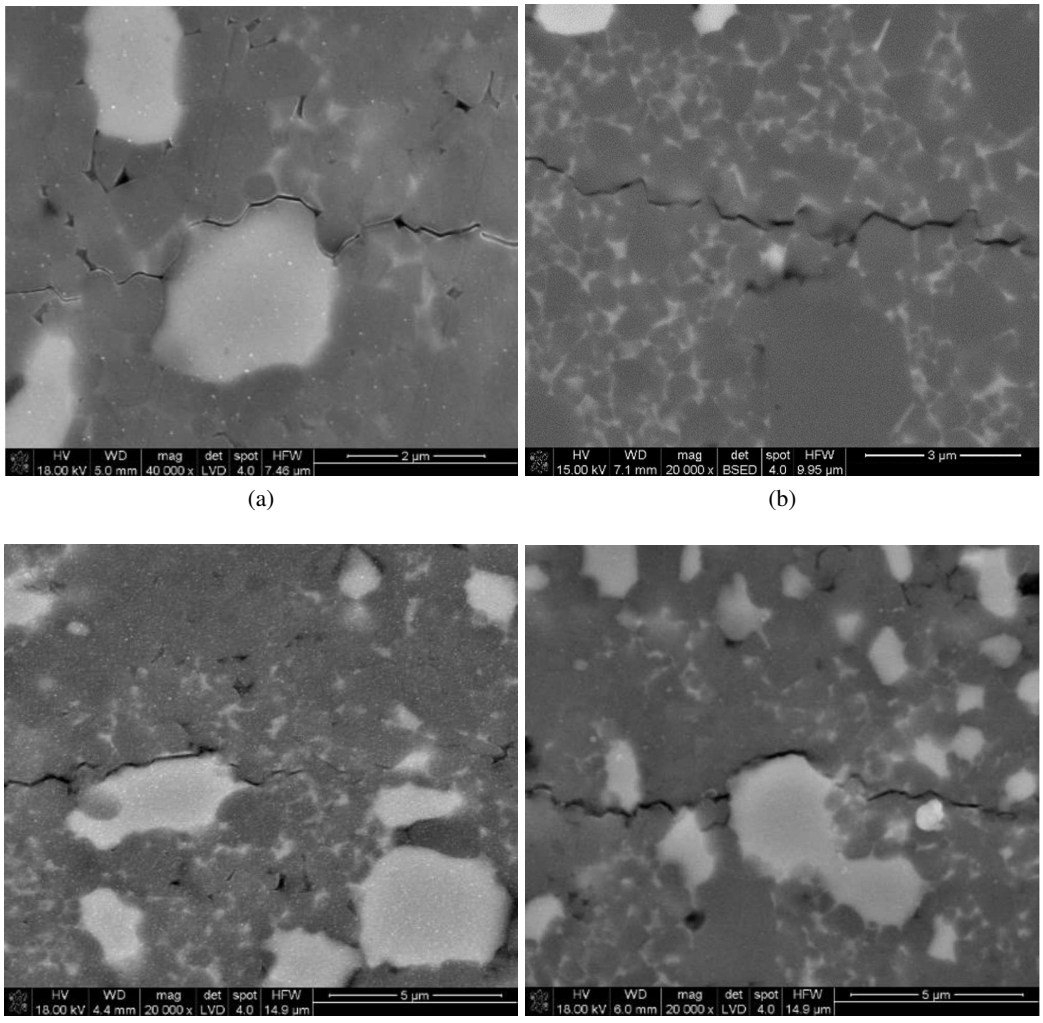

(a) (b)

(c) (d)

Figure 6. Mechanisms of effective increase in cracking energy in composites: a) SiC-0TiC, b)SiC-5TiC, c) SiC-10TiC and d) SiC-20TiC

Table 3. Comparison of actual data for main phases of composites components and the calculations by RVE model

Composite	Volume fraction of TiC [%]	Amount of inclusion grains
SiC-5TiC	5.1	100
SiC-10TiC	10.0	152
SiC-20TiC	20.1	190

other, which increase the size and shape inclusion variations (especially at higher volume fraction). The procedure of RVE filling with grains was iterated until the average inclusion size was close to that obtained from the quantitative microstructure analysis (Fig. 7) for subsequent composites. The values of the average equivalent grain diameter d_2 - in the two dimensions and the mean diameter of the grains D - in three dimensions for the TiC grains were calculated on the basis of the SEM micrographs and analysis of microstructure images. For this purpose, commercial software Aphelion was used. Such synthetic microstructures were composed of more

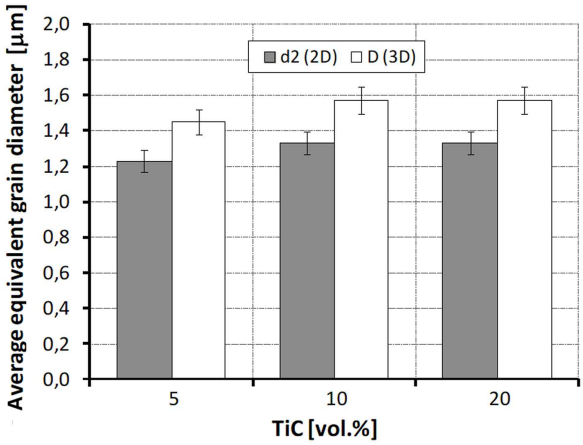

Figure 7. Calculation results of average equivalent diameter of TiC inclusions in two- and three-dimensional layout

than a hundred TiC grains distributed in a homogeneous matrix (Fig. 8).

The isotropic properties of component phase were assumed in calculations. Values applied for SiC were:

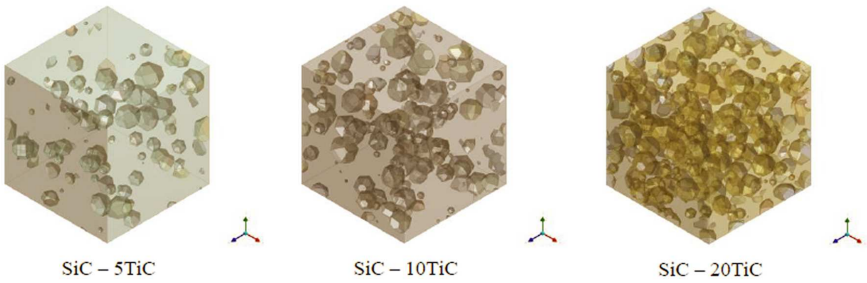

Figure 8. The appearance of modelled composite areas

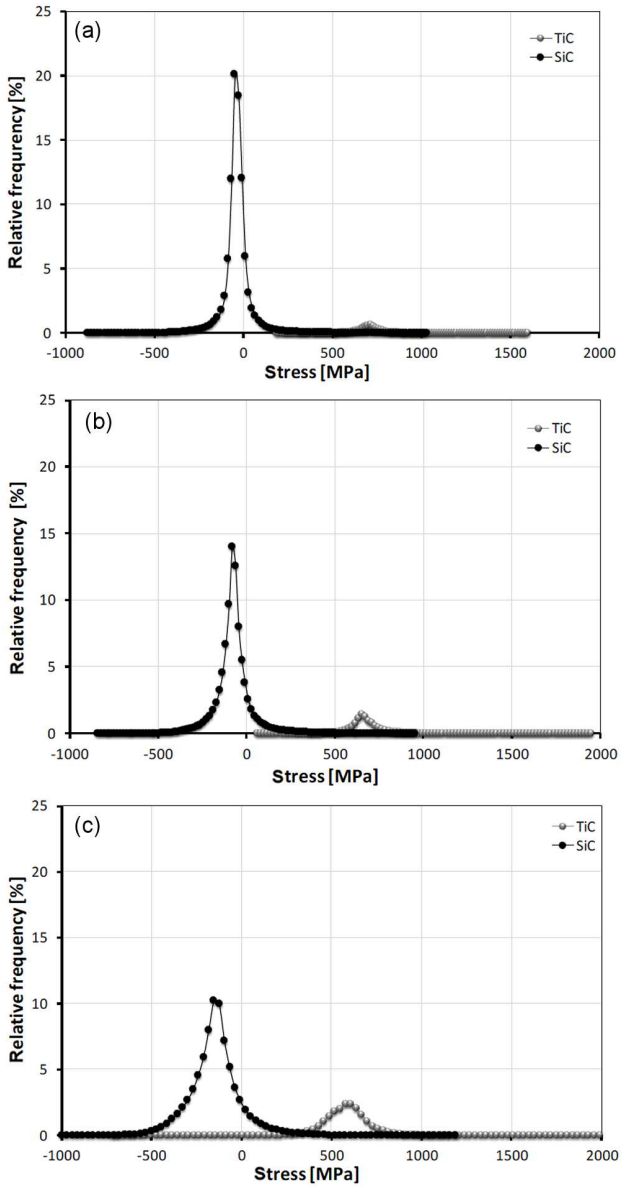

Figure 9. Distribution of normal stresses in the x direction for composites: a) SiC-5TiC, b) SiC-10TiC and c) SiC-20TiC

Young's modulus E_{SiC} = 415 GPa, Poisson's ratio ν_{SiC} = 0.16, linear thermal expansion coefficient in the range of 275–1275 K was $\alpha_{SiC} = 5.3 \cdot 10^{-6}\,K^{-1}$ [30]. The corresponding data for TiC were: E_{TiC} = 450 GPa, ν_{TiC} = 0.19 [31], $\alpha_{TiC} = 7.4 \cdot 10^{-6}\,K^{-1}$ [24]. The model assumed periodic boundary conditions that force the same degrees of freedom for the corresponding nodes lying on opposite edges of the RVE [32]. The models were thermally loaded by cooling at temperatures from 1273 to 273 K. It was assumed that at 1273 K thermal stresses are being relaxed by plastic and diffusion flow.

The results obtained for three composite systems by the FEM simulations indicate that with the increasing volume fraction of TiC phase, the residual thermal stresses increase in both the inclusion grains and the SiC matrix. Average values and distribution of the thermal stress calculated for the models are summarized in Table 4. They were expressed as hydrostatic stresses:

$$\sigma_h = \frac{\sigma_x + \sigma_y + \sigma_z}{3} \tag{1}$$

where σ_x, σ_y, σ_z are weighted averages of stresses (σ_{avg}) in directions x, y, z, calculated using following equation:

$$\sigma_{avg} = \sum \sigma_i \cdot x_i \tag{2}$$

where σ_i is value of the stress in the element i, in the selected direction in space and x_i is the volume fraction for element i.

The FEM simulations of thermal stresses showed that tensile stresses dominate in the TiC grains, regardless of their volume fraction and compressive stresses occur in the matrix. These stresses result from the difference in thermal expansion coefficients ($\alpha_{SiC} < \alpha_{TiC}$) of these phases. Analysis of the simulation results indicates that the increase in the volume fraction of the secondary phase (TiC) leads to the decrease in average value of stress but increases their spread (Fig. 9). For carbide matrix this is due to the increase in the volume fraction of the areas in which compressive stresses will prevail, what may improve fracture toughness. However, for the TiC phase, the spread of the stress distribution is related to the increase in the volume fraction of areas where

Table 4. Thermal stresses calculated in composites

Composite	σ_h of matrix [MPa]	σ_h of inclusions [MPa]
SiC-5TiC	−38 ± 148	713 ± 74
SiC-10TiC	−75 ± 167	674 ± 98
SiC-20TiC	−149 ± 200	593 ± 128

tensile stress is dominant. These areas are located near the interface. Because of the very high values of stresses present in the TiC grains, it can lead to the weakening of interface (grain boundary) strength and even cause microcracks [15]. The effect of this stress distribution is significantly decreased strength correlated with increasing amount of TiC addition.

IV. Conclusions

Dense composites with SiC matrix and homogeneous distribution of 5, 10 and 20 vol.% of TiC grains were prepared by hot-pressing at 2000 °C/0.5 h, under 25 MPa pressure and argon flow. Oxide activators from the Al_2O_3-Y_2O_3 system were used to densify SiC matrix.

In comparison to the reference sample (SiC sintered only with oxide additives), the Vickers hardness and fracture toughness slightly increase whereas bending strength significantly decreases. Among produced composites, the best mechanical properties had the composite with 5 vol.% TiC. With increasing volume fraction of TiC, an increase of residual thermal stresses in composites was observed. The calculated average internal stresses indicated possibility of microcracks creation at the grain boundaries. These phenomena would explain observed enhancement in the K_{Ic} values and decrease in the composite bending strength with the increased TiC fraction.

It is worth noting that there is no significant improvement of the mechanical properties of SiC-TiC composites in comparison with silicon carbide polycrystals sintered with oxide activators only.

Acknowledgements: The work was performed within statutory research realized on Faculty of Materials Science and Ceramics AGH University of Science and Technology, No. 11.11.160.617.

References

1. D. Bloor R.W. Cahn, *The Encyclopedia of Advanced Materials Vol.1, Silicon Carbide*, Elsevier Science Ltd., Cambridge, UK, 1994.
2. S. Prochazka, R.M. Scanlan, "Effect of boron and carbon on sintering of SiC", *J. Am. Ceram. Soc.*, **58** (1975) 72.
3. R.A. Alliegro, L.B. Coffin, J.R. Tinklepaugh, "Pressure-sintered silicon carbide", *J. Am. Ceram. Soc.*, **39** (1956) 386–389.
4. F.F. Lange, "Hot-pressing behavior of silicon carbide powders with additions of aluminum oxide", *J. Mater. Sci.*, **10** (1975) 314–320.
5. M. Omori, H. Takei, "Pressureless sintering of SiC", *J. Am. Ceram. Soc.*, **65** (1982) C-92.
6. K. Negita, "Effective sintering aids for silicon carbide ceramics: Reactivites of silicon carbide with various additives", *J. Am. Ceram. Soc.*, **69** (1986) C-308–C-310.
7. R.A. Cutler, T.B. Jackson, "Liquid phase sintered silicon carbide", pp. 309–318 in *Proceedings of 3rd International Symposium on Ceramic Materials and Components for Engines.* Am. Ceram. Soc., OH, USA, 1989.
8. E. Gomez, J. Echeberria, J. Iturriza, F. Castro, "Liquid phase sintering of SiC with additions of Y_2O_3, Al_2O_3 and SiO_2", *J. Eur. Ceram. Soc.*, **24** (2004) 2895–2903.
9. L. Stobierski, A. Gubernat, "Sintering of silicon carbide I. Effect of carbon", *Ceram. Int.*, **29** (2003) 287–292.
10. L. Stobierski, A. Gubernat, "Sintering of silicon carbide II. Effect of boron", *Ceram. Int.*, **29** (2003) 355–361.
11. A. Gubernat, L. Stobierski, P. Łabaj, "Microstructure and mechanical properties of silicon carbide pressureless sintered with oxide additives", *J. Eur. Ceram. Soc.*, **27** (2007) 781–789.
12. M.A. Janney, "Mechanical properties and oxidation behavior of a hot-pressed SiC-15 vol% TiB_2 composite", *Am. Ceram. Soc. Bull.*, **66** (1987) 322–324.
13. W.D.G. Boecker, S.G. Seshadri, J.S. Zanghi, J.E. Garnier, C.H. McMurtry, "Microstructure and material properties of SiC-TiB_2 particulate composites", *Am. Ceram. Soc. Bull.*, **66** (1987) 325–329.
14. H. Endo, M. Ueki, H. Kubo, "Microstructure and mechanical properties of SiC-TiC composites", *J. Mater. Sci.*, **26** (1991) 3769–3774.
15. C. Kyeong-Sik, K. Young-Wook, C. Heon-Jin, L. June-Gunn, "SiC-TiC and SiC-TiB_2 composites densified by liquid-phase sintering", *J. Mater. Sci.*, **31** (1996) 6223–6228.
16. C. Kyeong-Sik, C. Heon-Jin, L. June Gunn, K. Young-Wook, "Microstructure and fracture toughness of in-situ toughened SiC-TiC composites", *J. Mater. Sci. Lett.*, **17** (1998) 1081–1084.
17. L. Young-Il, K. Young-Wook, "Process-tolerant SiC-TiC composites", *J. Mater. Sci. Lett.*, **21** (2002) 863–866.
18. K. Young-Wook, L. Sung-Gu, L. Young-Il, "Pressureless sintering of SiC-TiC composites with improved fracture toughness", *J. Mater. Sci.*, **35** (2000) 5569–5574.
19. Y. Luo, S. Li, W. Pan, L. Li, "Fabrication and mechanical evaluation of SiC-TiC nanocomposites by SPS", *Mater. Lett.*, **58** (2003) 150–153.
20. J. Chen, W.J. Li, W. Jiang, "Characterization of sintered TiC-SiC composites", *Ceram. Int.*, **35** (2009) 3125–3129.
21. J. Cabrero, F. Audubert, R. Pailler, "Fabrication and characterization of sintered TiC-SiC composites", *J. Eur. Ceram. Soc.*, **31** (2011) 313–320.
22. D. Ahmoye, V.D. Krstic, "Reaction sintering of SiC composites with in situ converted TiO_2 to TiC", *J. Mater. Sci.*, **50** (2015) 2806–2812.
23. P. Auerkari, *Mechanical and Physical Properties of Engineering Alumina Ceramics*, Technical Research Centre of Finland, Espoo, Finland, 1996.
24. H.O. Pierson, *Handbook of Refractory Carbides and Nitrides*, William Andrew Publishing, Westwood, NJ, 1996.
25. H. Tulhoff, *Carbides*, Uhlman's Encyclopedia of Industrial Chemistry, Vol. A5, Weinheim, Germany, VCH, 1988.
26. L. Stobierski, *Silicon Carbide – Structure, Properties and Obtaining*, Ceramics 48, Polish Ceramic Society Publishing, Cracow, Poland, 1996 (in Polish).
27. A. Hyun-Gu, K. Young-Wook, L. June-Gunn, "Effect of initial α-phase content of SiC on microstructure and mechanical properties of SiC-TiC composites", *J. Eur. Ceram. Soc.*, **21** (2001) 93–98.
28. V. Kouznetsova, W.A.M. Brekelmans, F.P.T. Baaijens, "An approach to micro-macro modeling of heterogeneous materials", *Comput. Mech.*, **27** (2001) 37–48.
29. S. Kurukuri, *A Review of Homogenization Techniques for Heterogeneous Materials*, Weimar, Germany, 2004.

30. R.G. Munro, "Material properties of a sintered α-SiC", *J. Phys. Chem. Ref. Data*, **26** (1997) 1195–1203.
31. R. Chang, L.J. Graham, "Low-temperature elastic properties of ZrC and TiC", *J. Appl. Phys.*, **37** (1966) 3778–3783.
32. K. Terada, M. Hori, T. Kyoya, N. Kikuchi, "Simulation of the multi-scale convergence in computational homogenization approaches", *Int. J. Solids Struct.*, **37** (2000) 2285–2311.